Open access • Book Chapter • DOI:10.1007/3-540-34596-5_6

Adaptive Finite Element Approximation of Fluid-Structure Interaction Based on an Eulerian Variational Formulation — Source link

Thomas Dunne, Rolf Rannacher

Institutions: Heidelberg University

Published on: 06 Sep 2006

Topics: Eulerian path, Finite element method, Level set method, Method of mean weighted residuals and Fluid–structure interaction

European Conference on Computational Fluid Dynamics
ECCOMAS CFD 2006
P. Wesseling, E. Oñate and J. Périaux (Eds)

ADAPTIVE FINITE ELEMENT APPROXIMATION OF FLUID-STRUCTURE INTERACTION BASED ON AN EULERIAN VARIATIONAL FORMULATION

Th. Dunne*

* Institute of Applied Mathematics, University of Heidelberg, INF 294/293, 69120 Heidelberg, Germany
e-mail: thomas.dunne@iwr.uni-heidelberg.de,

Key words: fluid-structure interaction, Eulerian frame, initial position set method, level set method, a posteriori error estimation, DWR method, goal-oriented mesh adaptation

Abstract. *We propose a general variational framework for the adaptive finite element approximation of fluid-structure interaction problems. The modeling is based on an Eulerian description of the (incompressible) fluid as well as the (elastic) structure dynamics. This is achieved by tracking the movement of the initial positions of all 'material' points. In this approach the deformation appears as a primary variable in an Eulerian framework. Our approach uses a technique which is similar to the Level Set method in so far that it also tracks initial data, in our case the set of Initial Positions, and from this determines to which 'phase' a point belongs. To avoid the need for reinitialization of the initial position set, we employ the harmonic continuation of the structure velocity field into the fluid domain. Based on this monolithic model of the fluid-structure interaction we apply the dual weighted residual method for goal-oriented a posteriori error estimation and mesh adaptation to fluid-structure interaction problems. Results from nonstationary examples are presented.*

1 Introduction

In general most approaches to solving fluid-structure interaction problems can be categorized into two groups:

- The partitioned approach: in each time step separate the problems, solve each separately, and so converge iteratively to a solution, satisfying both equation and the interface conditions.
- The transformation approach: introduce an auxiliary unknown transformation function ζ_f for the time-dependent fluid domain based on the initial fluid domain. Then, all computations are done on the fixed reference domain and as part of the computation the auxiliary transformation function ζ_f has to be determined at each

time step. In a more general case this so-called 'arbitrary Lagrangian-Eulerian' (ALE) method uses a transformation function ζ_f that transforms the domains to an arbitrary domain and not the initial one.

Both, the partitioned and the transformation approach overcome the Euler-Lagrange discrepancy by explicitly tracking the fluid-structure interface by using mesh adjustment and are generally referred to as 'interface tracking' methods. Both methods leave the structure problem in its natural Lagrangian setting.

In this paper, we follow the alternative way of posing the fluid as well as the structure problem in a fully Eulerian framework. In the Eulerian setting a phase variable is employed on the fixed mesh to distinguish between the different phases, liquid and solid. This approach to identifying the fluid-structure interface is generally referred to as 'interface capturing', a method commonly used in the simulation of multiphase flows, [18]. Examples for the use of such a phase variable are the Volume of Fluid (VoF) method [14] and the Level Set (LS) method [8, 20, 23]. In the classical LS approach the distance function has to continually be reinitialized, due to the smearing effect by the convection velocity in the fluid domain. This makes the use of the LS method delicate for modeling FSI problems particularly in the presence of cornered structures. To cope with this difficulty, we propose a variant of the LS method that makes reinitialization unnecessary and which easily copes with cornered structures.

The method we describe does not depend on the specific structure model. The key variable in structure dynamics is the deformation, and since this depends on the deflection, it is understandable why structure dynamics is preferably described in the Lagrangian frame. To be able to describe the deformations in the Eulerian frame, we introduce the set of 'initial positions' (IP set) of all structure points. This set is then transported with the structure velocity in each time step. Based on the IP set points and their Eulerian coordinates the displacement is now available in an Eulerian sense. Also its gradient has to be rewritten appropriately. Since the fluid-structure interface will be crossing through cells, we will have to also transport the IP set in the fluid domain. For the convection of the IP set in the fluid domain we use a harmonic continuation of the structure velocity.

The equations we use are based on the momentum and mass conservation equations for the flow of an incompressible Newtonian fluid and the deformation of a compressible St. Venant-Kirchhoff solid. The spatial discretization is achieved using a second-order finite element method with conforming equal-order (bilinear) trial functions using 'local projection stabilization' as introduced by Becker and Braack [2, 3]. The time discretization uses the second-order 'Fractional-Step-θ' scheme originally proposed by Bristeau, Glowinski, and Periaux [6]. This method has the same complexity as the Crank–Nicolson scheme but better stability properties, [21].

Based on the Eulerian variational formulation of the FSI system, we use the 'dual weighted residual' (DWR) method, described in [4, 1], to derive 'goal-oriented' a posteriori error estimates. The evaluation of these error estimates requires the approximate solution of a linear dual variational problem. The resulting a posteriori error indicators are then

used for automatic local mesh adaption. The full application of the DWR method to FSI problems requires a Galerkin discretization in space as well as in time. Due to the use of a difference scheme in time, in this paper we are limited to 'goal-oriented' mesh adaptation of the quasi-steady states within the time stepping process.

The self-induced oscillation of a thin elastic bar immersed in an incompressible fluid is treated (FLUSTRUK-A benchmark described in [15]). For this test problem, our method is compared against a standard 'arbitrary Lagrange Eulerian' (ALE) approach. The possible potential of the fully Eulerian formulation of the FSI problems is indicated by its good behavior for large structure deformations. All computations and visualizations are done using the flow-solver package GASCOIGNE [28] and the graphics package VISUSIMPLE [27]. More details on the software implementation can be found in [9].

The outline of this paper is as follows. Section 2 introduces the basic notation for the Eulerian formulation of the FSI problem which is then presented in Section 3. Section 4 presents the discretization in space and time and the derivation of a posteriori error estimates and strategies for mesh adaptation. Finally, Section 5 contains the results obtained for the nonstationary benchmark problem FLUSTRUK-A (oscillations of a thin elastic bar) for various combinations of material models and flow conditions.

2 Notation

We begin with introducing some notation which will be used throughout the paper. By $\Omega \subset \mathbb{R}^d$ ($d = 2$ or $d = 3$), we denote the domain of definition of the FSI problem. The domain Ω is supposed to be *time independent* but to consist of two possibly time-dependent subdomains, the fluid domain $\Omega_f(t)$ and the structure domain $\Omega_s(t)$. Unless needed, the explicit time dependency will be skipped in this notation. The boundaries of Ω, Ω_f, and Ω_s are denote by $\partial\Omega$, $\partial\Omega_f$, and $\partial\Omega_s$, respectively. The common interface between Ω_f and Ω_s is $\Gamma_i(t)$, or simply Γ_i.

The initial structure domain is denoted by $\widehat{\Omega}_s$. Spaces, domains, coordinates, values (such as pressure, displacement, velocity) and operators associated to $\widehat{\Omega}_s$ (or $\widehat{\Omega}_f$) will likewise be indicated by a 'hat'.

Partial derivatives of a function f with respect to the $i-$th coordinate are denoted by $\partial_i f$, and the total time-derivative by $d_t f$. The divergences of vectors and tensors are written as $\mathrm{div} f = \sum_i \partial_i f_i$ and $(\mathrm{div} F)_i = \sum_j \partial_j F_{ij}$. The gradient of a vector valued function v is the tensor $(\nabla v)_{ij} = \partial_j v_i$.

By $[f]$, we denote the jump of a (possibly discontinuous) function f across an interior boundary, where n is always the unit vector n at points on that boundary.

For a set X, we denote by $L^2(X)$ the Lebesque space of square-integrable functions on X equipped with the usual inner product and norm

$$(f,g)_X := \int_X fg\, dx, \quad \|f\|_X^2 = (f,f)_X,$$

respectively, and correspondingly for vector- and matrix-valued functions. Mostly the

domain X will be Ω, in which case we will skip the domain index in products and norms. For Ω_f and Ω_s, we similarly indicate the associated spaces, products, and norms by a corresponding index 'f' or 's'.

Let $L_X := L^2(X)$ and $L^0_X := L^2(X)/\mathbb{R}$. The functions in L_X (with $X = \Omega$, $X = \Omega_f(t)$, or $X = \Omega_s(t)$) with first-order distributional derivatives in L_X make up the Sobolev space $H^1(X)$. Further, $H^1_0(X) = \{v \in H^1(X) : v_{|\partial X_D} = 0\}$, where ∂X_D is that part of the boundary ∂X at which Dirichlet boundary conditions are imposed. Further, we will use the function spaces $V_X := H^1(X)^d$, $V^0_X := H^1_0(X)^d$, and for time-dependent functions

$$\begin{aligned} \mathcal{L}_X &:= L^2[0,T;L_X], \quad \mathcal{V}_X := L^2[0,T;V_X] \cap H^1[0,T;V^*_X], \\ \mathcal{L}^0_X &:= L^2[0,T;L^0_X], \quad \mathcal{V}^0_X := L^2[0,T;V^0_X] \cap H^1[0,T;V^*_X], \end{aligned}$$

where V^*_X is the dual of V^0_X. Again, the X-index will be skipped in the case of $X = \Omega$, and for $X = \Omega_f$ and $X = \Omega_s$ a corresponding index 'f' or 's' will be used.

3 Formulation

In this section, we introduce the Eulerian formulation of the FSI problem. We introduce the fluid and structure models in the respective domains and with respective boundary conditions. The domains and boundary conditions are later unified. For the sake of brevity we write down the final complete model for fluid-structure interaction governed by the equations for conservation of mass and momentum. A detailed explanation of how this model is derived can be found in our previous paper [10].

3.1 Fluid

For the liquid part, we assume a Newtonian incompressible fluid governed by the usual Navier-Stokes equations, i.e., the equations describing conservation of mass and momentum. The (constant) density and kinematic viscosity of the fluid are ρ_f and ν_f, respectively. The equations are posed in an Eulerian framework in the time-dependent domain $\Omega_f(t)$. The physical unknowns are the scalar pressure field $p_f \in \mathcal{L}_f$ and the vector velocity field $v_f \in v^D_f + \mathcal{V}_f$. Here, v^D_f is a suitable extension of the prescribed Dirichlet data on the boundaries (both moving or stationary) of Ω_f, and g_1 is a suitable extension to all of $\partial\Omega_f$ of the Neumann data for $\sigma_f \cdot n$ on the boundaries. We 'hide' the fluid-structure interface conditions of steadiness of velocity and normal stress in parts of the boundary conditions v^D_f and g_1. These are addressed in Section 3.2.1, below.

3.2 Structure

The density of the structure is ρ_s. The material elasticity is usually described by a set of two parameters, the Poisson ratio ν_s and the Young modulus E_s, or alternatively, the

Lamé coefficients λ_s and μ_s. These parameters satisfy the following relations:

$$\nu_s = \frac{\lambda_s}{2(\lambda_s+\mu_s)}, \quad E_s = \mu_s\frac{3\lambda_s+2\mu_s}{\lambda_s+\mu_s}, \quad \mu_s = \frac{E_s}{2(1+\nu_s)}, \quad \lambda_s = \frac{\nu_s E_s}{(1+\nu_s)(1-2\nu_s)},$$

where $\nu_s = \frac{1}{2}$ for incompressible and $\nu_s < \frac{1}{2}$ for compressible material.

We consider a compressible elastic material described by the St. Venant-Kirchhoff (STVK) model governed by the equations for conservation of mass and momentum. Usually these equations are formulated in Lagrangian coordinates in the domain $\hat{\Omega}_s$ with the vector displacement and velocity fields $\hat{u}_s \in \hat{u}^D + \hat{\mathcal{V}}_s^0$, $\hat{v}_s \in \hat{v}_s^D + \hat{\mathcal{V}}_s^0$. Here, $\hat{u}^D$ and $\hat{v}_s^D$ are suitable extensions of the prescribed Dirichlet data on the boundaries of $\hat{\Omega}_s$, and $\hat{g}_2$ is a suitable extension to all of $\partial\hat{\Omega}_s$ of the Neumann data for $\hat{\sigma}_s \cdot n$ on the boundaries. Again, similarly as for the fluid problem, we 'hide' the fluid-structure interface conditions of steadiness of velocity and normal stress in parts of the boundary conditions $\hat{v}_s^D$ and $\hat{g}_2$. These are addressed in Section 3.2.1, below.

For the sake of simplicity, we assume that the only boundary displacements that take place are on $\hat{\Gamma}_i$, i.e.,

$$\hat{u}^D = \hat{v}_s^D = 0 \text{ on } \partial\hat{\Omega}_s \setminus \hat{\Gamma}_i.$$

3.2.1 Combination to a unified Eulerian frame

By rewriting the structure equations into an Eulerian frame, both the fluid and the structure equations can be combined into one unified formulation. This is achieved mainly by introducing the *'set of initial positions'* (IP set) $\phi(\Omega)$ of all points of Ω at time t. If we look at a given 'material' point at the position $x \in \Omega$ and the time $t \in (0,T]$, then the value $\phi(t,x)$ will tell us what the initial position of this point was at time $t = 0$. These points are transported in the full domain with a certain velocity w. The convection velocity in the structure will be the structure velocity itself, $w_{|\Omega_s} = v_s$. In the fluid domain we use the harmonic continuation of the structure velocity to the whole domain Ω, which is likewise denoted by w.

The steadiness of velocity across the fluid-structure interface Γ_i is strongly enforced by requiring one common continuous field for the velocity on Ω. The Dirichlet boundary data v_f^D and v_s^D on parts of $\partial\Omega$ are merged into a suitable velocity field $v^D \in V$. Finally, the force balance condition $\sigma_f \cdot n = \sigma_s \cdot n$ on Γ_i now appears as a boundary integral of the jump $[\sigma \cdot n]$ on the right hand side,

$$([\sigma \cdot n], \psi^v)_{\Gamma_i} = \int_{\Gamma_i} (\sigma_f - \sigma_s) \cdot n_f \psi^v \, do.$$

By omitting this boundary integral the (weak) continuity of $\sigma \cdot n$ becomes an implicit condition of the combined variational formulation. The remaining parts of the Neumann data g_1 and g_2 now form the Neumann boundary data on $\partial\Omega$ and are combined to g_3.

Again, we refer to the previous paper [10] which contains a detailed explanation of how this model is derived.

3.3 Eulerian formulation of the FSI problem

Find fields $\{v, w, u, p\} \in \{v^D + \mathcal{V}^0\} \times \mathcal{V}^0 \times \mathcal{V}^0 \times \mathcal{L}$, *such that* $v(0) = v^0$, $u(0) = u^0$, *and*

$$\begin{aligned} (\rho(\partial_t v + v \cdot \nabla v), \psi) + (\sigma, \epsilon(\psi)) &= (g_3, \psi)_{\partial\Omega} + (f_3, \psi) \quad \forall \psi \in V^0, \\ (\chi_f \mathrm{div} v, \chi) + (\chi_s \alpha_p \nabla p, \nabla \chi) &= 0 \quad \forall \chi \in L, \\ (\partial_t u - w + w \cdot \nabla u, \psi) &= 0 \quad \forall \psi \in V^0, \\ (\chi_s (w - v), \psi) + (\chi_f \alpha_w \nabla w, \nabla \psi) &= 0 \quad \forall \psi \in V^0, \end{aligned} \tag{1}$$

where α_p is a small positive constant, $\rho := \chi_f \rho_f + \chi_s \rho_s$ and $\sigma := \chi_f \sigma_f + \chi_s \sigma_s$, with

$$\chi_f := \begin{cases} 1, & x - u \in \hat{\Omega}_f \setminus \hat{\Gamma}_i, \\ 0, & x - u \in \hat{\Omega}_s, \end{cases} \qquad \chi_s = 1 - \chi_f,$$

and

$$\begin{aligned} \sigma_f &:= -pI + 2\rho_f \nu_f \epsilon(v), \\ \sigma_s &:= J^{-1} F (\lambda_s (\mathrm{tr} E) I + 2\mu_s E) F^T \\ F &:= (I - \nabla u)^{-1}, \quad J := \det F, \quad E := \tfrac{1}{2}(F^T F - I). \end{aligned}$$

In this variational formulation the position of the fluid structure interface Γ_i is implicitly given by the displacement u and the characteristic function χ_s,

$$\Gamma_i(t) = \{x \in \Omega,\ x - u(x,t) \in \hat{\Gamma}_i\}. \tag{2}$$

Notice that the system (1) is *nonlinear* even if the two subproblems are linear, e.g., for a Stokes fluid interacting with a linear elastic structure.

4 Discretization

In this section, we detail the discretization in space and time of the FSI problem based on its Eulerian variational formulation (1).

4.1 Mesh notation

The spatial discretization is achieved by using a conforming finite element Galerkin method on meshes $\mathbb{T}_h$ consisting of cells denoted by K, which are (convex) quadrilaterals in 2d or hexaedrals in 3d. The mesh parameter h is a scalar cell-wise constant function defined by $h_{|K} := h_K = \mathrm{diam}(K)$. 'Refinement' of cells is always by bisection, i.e., by joining opposite midpoints (or midedges) of sides or faces. 'Coarsening' of a cell is possible if it has been generated by prior refinement of some 'parent cell'. The 'finest level' of cells of a mesh $\mathbb{T}_h$ consists of all cells that can be removed by coarsening in one sweep. The resulting coarsened mesh is referred to as $\mathbb{T}_{2h}$. To facilitate mesh refinement and

coarsening, we allow the cells to have a certain number of nodes that are at the midpoint of sides or faces of neighboring cells. These 'hanging nodes' do not carry degrees of freedom and the corresponding function values are determined by linear or bilinear interpolation of neighboring 'regular' nodal points. For more details on this approach see [7] or [1].

4.2 Galerkin formulation

For arguments $U = \{v, w, u, p\}$ and $\Psi = \{\psi^v, \psi^w, \psi^u, \psi^p\} \in \mathcal{W} := \mathcal{V} \times \mathcal{V} \times \mathcal{V} \times \mathcal{V}$, we introduce the space-time semilinear form

$$\begin{aligned} A(U)(\Psi) \;:=\; \int_0^T \Big\{ & (\rho(\partial_t v + v \cdot \nabla v), \psi^v) + (\sigma(U), \epsilon(\psi^v)) \\ & + (\chi_f \mathrm{div} v, \psi^p) + (\chi_s \alpha_p \nabla p, \nabla \psi^p) \\ & - (g_3, \psi^v)_{\partial\Omega} - (f_3, \psi^v) + (\partial_t u - w + w \cdot \nabla u, \psi^u) \\ & + (\chi_s (w - v), \psi^w) + (\chi_f \alpha_w \nabla w, \nabla \psi^w) \Big\}\, dt. \end{aligned}$$

With this notation, we can write the variational problem (1) in compact form: *Find* $U \in U^D + \mathcal{W}^0$ *, such that*

$$A(U)(\Psi) = 0 \quad \forall \Psi \in \mathcal{W}^0, \tag{3}$$

where U^D *is an appropriate extension of the Dirichlet boundary and initial data and the space* $\mathcal{W}^0$ *is defined by*

$$\mathcal{W}^0 := \{\Psi \in \mathcal{V}^0 \times \mathcal{V}^0 \times \mathcal{V}^0 \times \mathcal{V}^0,\ \psi^u(0) = \psi^v(0) = 0\}.$$

For discretizing this problem in space, we use equal-order Q_1 finite elements (d-linear shape functions) for all unknowns, where the corresponding finite element spaces are denoted by $L_h \subset L$, $V_h \subset V$, $W_h \subset W$, etc.. Within the present abstract setting the discretization in time is likewise thought as by a Galerkin method, such as the dG(r) ('discontinuous' Galerkin) or the cG(r) ('continuous' Galerkin) method. Here, the dG(0) method is closely related to the backward Euler scheme and the dG(1) method to the Crank–Nicolson scheme. However, in the test computations described below, we have used a Galerkin method only in space but finite difference schemes in time. The full space-time Galerkin framework is mainly introduced as basis for a systematic approach to residual-based a posteriori error estimation as described below.

The spatial discretization by 'equal-order' finite elements for velocity and pressure needs stabilization in order to compensate for the missing 'inf-sup stability'. We use the so-called *'local projection stabilization'* (LPS) introduced by Becker and Braack [2, 3]. An analogous approach is also employed for stabilizing the convection in the flow model as well as in the transport equation for the displacement u. We define the mesh-dependent

bilinear form

$$(\varphi,\psi)_\delta := \sum_{K\in\mathbb{T}_h} \delta_K\,(\varphi,\psi)_K,$$
$$\delta_K := \alpha\big(\chi_f\rho_f\nu_f h_K^{-2} + + \beta\rho|v_h|_{\infty;K}h_K^{-1} + \gamma|w_h|_{\infty;K}h_K^{-1}\big)^{-1}.$$

Further, we introduce the 'fluctuation operator' $\pi_h : V_h \to V_{2h}$ on the finest mesh level $\mathbb{T}_h$ by $\pi_h = I - P_{2h}$, where $P_{2h} : V_h \to V_{2h}$ is the L^2-projection. The operator π_h measures the fluctuation of a function in V_h with respect to its projection into the next coarser space V_{2h}. With this notation, we define the stabilization form

$$\begin{aligned} S_\delta(U_h)(\Psi_h) \;:=\; \int_0^T \Big\{ &(\nabla\pi_h p_h, \nabla\pi_h\psi_h^p)_\delta + (\rho v_h\cdot\nabla\pi_h v_h, v_h\cdot\nabla\pi_h\psi_h^v)_\delta \\ &+ (w_h\cdot\nabla\pi_h u_h, w_h\cdot\nabla\pi_h\psi_h^u)_\delta\Big\}\,dt, \end{aligned}$$

where the first term of δ_K stabilizes the fluid pressure, the second one the transport in the flow model, and the third one the transport of the displacement u_h. Then, the stabilized Galerkin approximation of problem (3) reads: *Find* $U_h \in U_h^D + \mathcal{W}_h^0$, *such that*

$$A_\delta(U_h)(\Psi_h) := A(U_h,\Psi_h) + S_\delta(U_h)(\Psi_h) = 0, \quad \forall\Psi_h \in \mathcal{W}_h^0. \tag{4}$$

The LPS has the important property that it acts only on the diagonal terms of the coupled system and that it does not contain any second-order derivatives. However, it is only 'weakly' consistent, as it does not vanish for the continuous solution, but it tends to zero with the right order as $h \to 0$. The choice of the numbers α,β,γ in the stabilization parameter δ_K is, based on practical experience, in our computations $\alpha = 1/2$, and $\beta = \gamma = 1/6$.

4.3 Time discretization

The discretization in time is by the so-called *'fractional-step-θ scheme'* in which each time step $t_{n-1} \to t_n$ is splitted into three substeps $t_{n-1} \to t_{n-1+\theta} \to t_{n-\theta} \to t_n$.

The *'fractional-step-θ scheme'* is a less dissipative scheme than most of the other second-order implicit schemes and therefore suitable for computing oscillatory solutions; for more details, we refer to [21], [22], and [11].

4.4 Solution of the algebraic systems

After time and space discretization, in each substep of the fractional-step-θ scheme (or any other fully implicit time-stepping scheme) a quasi-stationary nonlinear algebraic system has to be solved. This is done by a standard Newton-type method with adaptive step-length selection. The resulting linear subproblems are then solved by the GMRES method with preconditioning by a geometric multigrid method with block-ILU smoothing. This approach is well known, we omit its details and refer to the relevant literature, e.g., [25], [21], or [16].

4.5 Mesh adaptation

Now, we come to the main issues of this paper, namely the automatic mesh adaptation within the finite element solution of the FSI problem. The computations shown in Section 5, below, have been done on two different types of meshes:

- locally refined meshes obtained using a purely geometry-based criterion by marking all cells for refinement which have certain prescribed distances from the fluid-structure interface,
- locally refined meshes obtained using a systematic residual-based criteria by marking all cells for refinement or coarsening which have error indicators above or below a certain threshold.

The main goal of this project is to employ the *'dual weighted residual method'* (DWR method) for the adaptive solution of FSI problems. This method is explained in [4] (see also [1]) as an extension of the duality technique for a posteriori error estimation described in [12]. The DWR method provides a general framework for the derivation of 'goal-oriented' a posteriori error estimates together with criteria of mesh adaptation for the Galerkin discretization of general linear and nonlinear variational problems, including optimization problems. It is based on a complete *variational* formulation of the problem, such as (3) for the FSI problem. In fact, this was one of the driving factors for deriving the Eulerian formulation underlying (3). In order to incorporate also the time discretization into this framework, we have to use a fully space-time Galerkin method, i.e., a standard finite element method in space combined with the dG(r) od cG(r) ('discontinuous' Galerkin or 'continuous' Galerkin) method in time. The following discussion assumes such a space-time Galerkin discretization, though in our test computations, we have used the fractional-step-θ scheme which is a difference scheme. Accordingly, in this paper the DWR method is used only in its stationary form in computing intermediate quasi-steady states within the time stepping process.

We begin with the description of the DWR method for the special case of an FSI problem governed by an abstract variational equation such as (3). For notational simplicity, we think the nonhomogeneous boundary and initial data U^D to be incorporated into a linear forcing term $F(\cdot)$, or to be exactly representable in the approximating space $\mathcal{W}_h$. Then, the problem reads as follows: *Find* $U \in U^D + \mathcal{W}^0$, *such that*

$$A(U)(\Psi) = F(\Psi) \quad \forall \Psi \in \mathcal{W}^0. \tag{5}$$

The corresponding (stabilized) Galerkin approximation reads: *Find* $U_h \in U_h^D + \mathcal{W}_h$, *such that*

$$A(U_h)(\Psi_h) + S_\delta(U_h)(\Psi_h) = F(\Psi) \quad \forall \Psi_h \in \mathcal{W}_h^0. \tag{6}$$

Suppose now that the goal of the computation is the evaluation of the value $J(U)$ for some functional $J(\cdot)$ which is defined on $\mathcal{W}$ and (for notational simplicity only) assumed as

linear. We want to control the quality of the discretization in terms of the error $J(U-U_h)$. To this end, we introduce the directional derivative

$$A'(U)(\Phi,\Psi) := \lim_{\epsilon\to 0}\frac{1}{\epsilon}\big\{A(U+\epsilon\Phi)(\Psi) - A(U)(\Psi)\big\}, \quad \Phi,\Psi\in\mathcal{W}^0,$$

the existence of which is assumed.

With the above notation, we introduce the bilinear form

$$L(U,U_h)(\Phi,\Psi) := \int_0^1 A'(U_h+s(U-U_h))(\Phi,\Psi)\,ds,$$

and formulate the 'dual problem'

$$L(U,U_h)(\Phi,Z) = J(\Phi) \quad \forall\Phi\in\mathcal{W}^0. \tag{7}$$

In the present abstract setting the existence of a solution $Z\in\mathcal{W}^0$ of the dual problem (7) has to be assumed. Now, taking $\Phi = U-U_h\in\mathcal{W}^0$ in (7) and using the Galerkin orthogonality property

$$A(U)(\Psi_h) - A(U_h)(\Psi_h) = S_\delta(U_h)(\Psi_h), \quad \Psi\in\mathcal{W}_h^0,$$

yields the error representation

$$\begin{aligned}
J(U-U_h) &= L(U,U_h)(U-U_h,Z)\\
&= \int_0^1 A'(U_h+s(U-U_h))(U-U_h,Z)\,ds\\
&= A(U)(Z) - A(U_h)(Z)\\
&= F(Z-\Psi_h) - A(U_h)(Z-\Psi_h) - S_\delta(U_h)(\Psi_h)\\
&=: \rho(U_h)(Z-\Psi_h) - S_\delta(U_h)(\Psi_h),
\end{aligned}$$

where $\Psi_h\in\mathcal{W}^0$ is an arbitrary element, usually taken as the generic nodal interpolant $I_hZ\in\mathcal{W}_h^0$ of Z. For the evaluation of the terms on the right-hand side, we split the integrals in the residual term $\rho(U_h)(Z-\Psi_h)$ into their contribution from the single mesh cells $K\in\mathbb{T}_h$ and integrate by parts. This results in an estimate of the error $|J(U-U_h)|$ in terms of computable local residual terms $\rho_K(U_h)$ multiplied by certain weight factors $\omega_K(Z)$ which depend on the dual solution Z,

$$|J(U-U_h)| \le \sum_{K\in\mathbb{T}_h}\rho_K(U_h)\,\omega_K(Z) + |S_\delta(U_h)(\Psi_h)|. \tag{8}$$

Since the dual solution Z is unknown, the evaluation of the weights $\omega_K(Z)$ requires further approximation. We linearize by assuming

$$L(U,U_h)(\Phi,\Psi)\approx L(U_h,U_h)(\Phi,\Psi) = A'(U_h)(\Phi,\Psi)$$

and use the approximate 'discrete' dual solution $Z_h \in \mathcal{W}_h^0$ defined by

$$A'(U_h)(\Phi, Z_h) = J(\Phi_h) \quad \forall \Phi_h \in \mathcal{W}_h^0. \tag{9}$$

From Z_h, we generate improved approximations to Z in a post-processing step by patch-wise higher-order interpolation. For example in 2d, on 2×2-patches of cells in $\mathbb{T}_h$ the 9 nodal values of the piecewise bilinear Z_h are used to construct a patchwise biquadratic function $\tilde{Z}$. This is then used to obtain the approximate error estimate

$$|J(U - U_h)| \approx \eta := \sum_{K \in \mathbb{T}_h} \rho_K(U_h)\, \omega_K(\tilde{Z}) \tag{10}$$

which is the basis of automatic mesh adaptation, [5, 1].

4.5.1 Mesh adaptation algorithm.

The approach we use for the adaptive refinement and coarsening of the spatial mesh is straightforward. The goal here is to keep the number of cells below a given threshold N_{max}. On the basis of the (approximate) a posteriori error estimate (10), the mesh adaptation proceeds as follows:

1. Compute the primal solution U_h from (6) on the current mesh, starting from some initial state, e.g., that with zero deformation.
2. Compute the solution $\tilde{Z}_h$ of the approximate discrete dual problem (9).
3. Evaluate the cell-error indicators $\eta_K := \rho_K(U_h)\, \omega_K(\tilde{Z}_h)$.
4. Determine the cells whose error indicators are above and 50% below the average error indicator value. The cells of the second group are coarsened and if the number of cells is below N_{max} then only so many of the cells of the first group are refined (in order of η_K) so that the resulting number of cells is below N_{max}. Then, continue with Step 1.

5 Numerical test 3: FSI benchmark FLUSTRUK-A

We use the FSI benchmark FLUSTRUK-A described in [15]. A thin elastic bar immersed in an incompressible fluid develops self-induced time-periodic oscillations of different amplitude depending on the material properties assumed. In order to have a fair comparison of our Eulerian-based method with the traditional Eulerian-Lagrangian approach, we have also implemented an ALE method for this benchmark problem.

The configuration of this benchmark shown in Figure 1 is based on the successful CFD benchmark 'flow around a cylinder', [26].

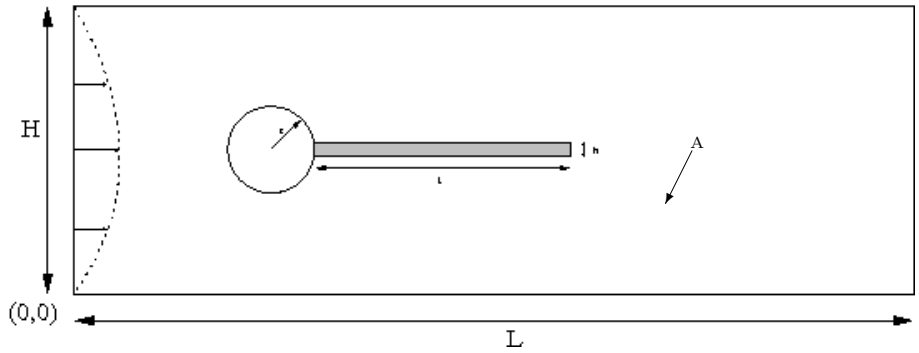

Figure 1: Configuration of the FSI benchmark 'FLUSTRUK-A'.

Configuration: $L = 2.5,\ H = 0.41$, left bottom corner at $(0, 0)$. The center of the circle is positioned at $C = (0.2, 0.2)$ with radius $r = 0.05$. The elastic bar has length $l = 0.35$ and height $h = 0.02$. Its right lower end is at $(0.6, 0.19)$ and its left end is clamped to the circle. The control point $A(t)$ is fixed at the trailing edge of the structure with $A(0) = (0.6, 0.20)$.

Boundary and initial conditions: Along the upper and lower boundary the 'no-slip' condition is used for the velocity. At the (left) inlet a constant parabolic inflow profile, $v(0, y) = 1.5\,\bar{U}\,\frac{4y(H-y)}{H^2}$, is prescribed, and at the (right) outlet zero-stress $\sigma \cdot n = 0$ is realized by using the 'do-nothing' approach in the variational formulation, [13, 21]. The initial condition is zero flow velocity and structure displacement.

Material properties: The fluid is assumed as incompressible and Newtonian, the cylinder as fixed and rigid, and the structure as (compressible) St. Venant-Kirchhoff (STVK) type. The following test cases are considered:

- *FSI test:* A configuration is treated with a prescribed inflow velocity and material stiffness parameter; the Eulerian approach is compared to the standard ALE method. A uniform time-step size of $0.005\,s$ is used.
- *FSI with large deflections:* The fluid is set to be initially in rest around the bar. The gravitational force on the bar is very large, causing a large deformation of the bar and eventually it reaching and running up against the channel wall. We compare results obtained from coarse heuristic meshes, refined heuristic meshes and meshes obtained using the DWR methods. This case is difficult for the ALE method but can easily be handled by the Eulerian approach.

5.1 FSI test

The parameters are chosen such that a visible transient behavior of the bar can be seen. To ensure a 'fair' comparison of results, we calculate the comparison values using the ALE method.

Table 1: Parameter settings for the FSI test cases.

parameter	FSI-2	FSI-2*
structure model	STVK	STVK
$\rho_f[10^3 kg\, m^{-3}]$	1	1
$\nu_f[10^{-3} m^2 s^{-1}]$	1	1
ν_s	0.4	0.4
$\rho_s[10^3 kg\, m^{-3}]$	10	20
$\mu_s[10^6 kg\, m^{-1} s^{-2}]$	0.5	0.5
$U[m\, s^{-1}]$	1	0

Some snapshots of the results of this simulation are shown in Figure 2. The time-dependent behavior of the displacements for the tests are shown in Figure 3.

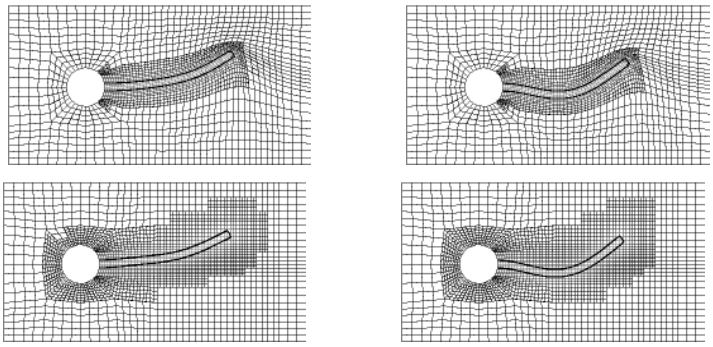

Figure 2: FSI-2: Snapshots of results obtained by the ALE (top two) and by the Eulerian (bottom two) approaches.

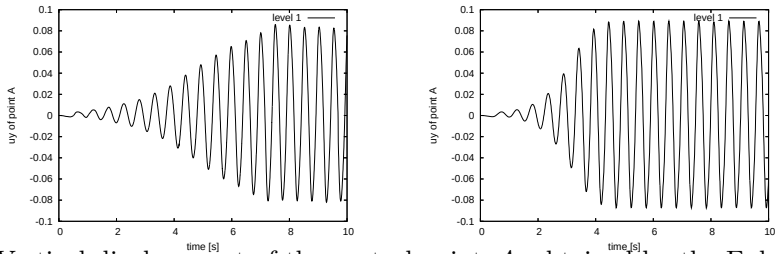

Figure 3: FSI-2: Vertical displacement of the control point A, obtained by the Eulerian approach (left, $N = 2082$ cells) with maximum amplitude $2.226 \cdot 10^{-2}$ and frequency $1.92\, s^{-1}$, and by the ALE approach (right, $N = 2784$ cells) with maximum amplitude $2.68 \cdot 10^{-2}$ and frequency $1.953\, s^{-1}$.

5.2 FSI test with large deformations

In the test case FSI-2* (see Table 1) the fluid is initially in rest and the bar is subjected to a vertical force. This causes the bar to bend downward until it touches the bottom wall. A sequence of snapshots of the transition to steady state obtained by the Eulerian approach for this problem is shown in Figure 4. The position of the trailing tip A is show in Figure 5.

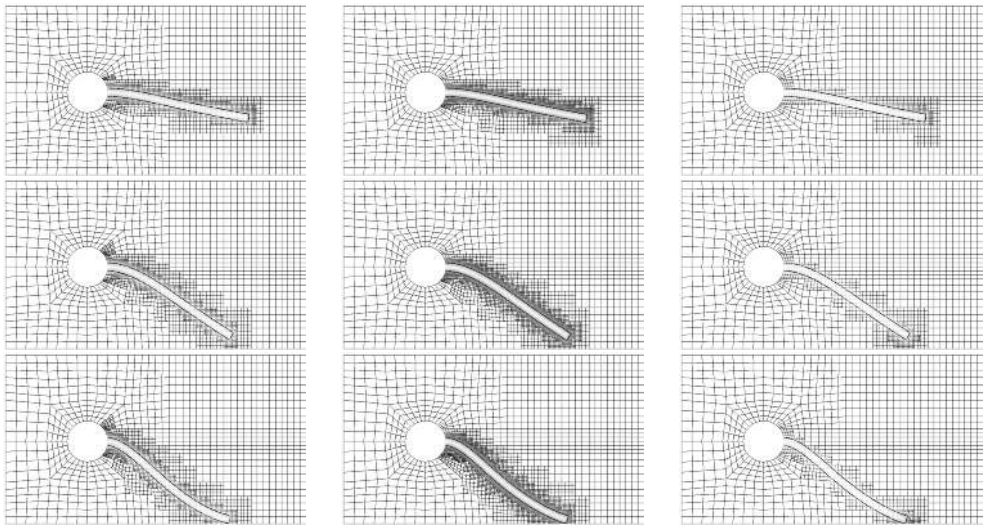

$N \sim 3,000$ $N \sim 12,000$ $N \sim 1,900$

Figure 4: A sequence of snap-shots of the bar's large deformation under gravitational loading obtained by the Eulerian approach.

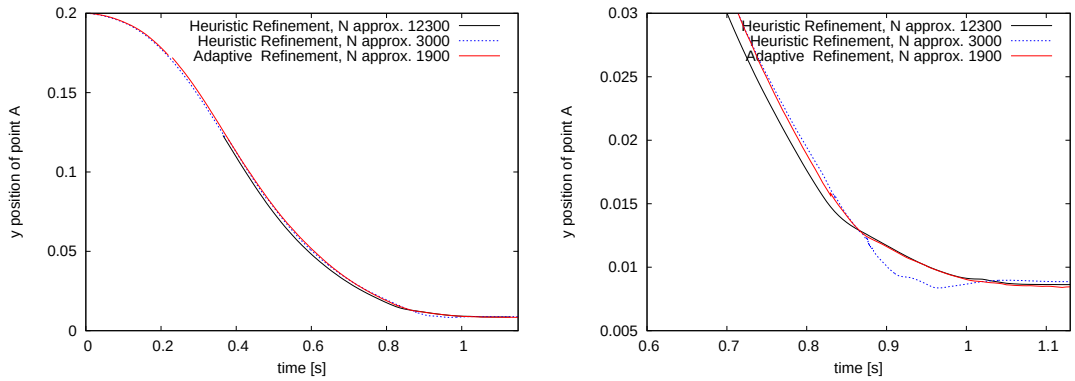

Figure 5: Position $x_A(t)$ of point A, CPU-time: heuristic refinement: 30h, adaptive refinement: 4h

6 Summary and future development

In this paper we presented a fully Eulerian variational formulation for 'fluid-structure interaction' (FSI) problems. This approach uses the 'initial position' set (IP set) method for interface capturing, which is similar to the 'level set' (LS) method, but preserves sharp corners of the structure. The harmonic continuation of the structure velocity avoids the need of reinitialization of the IP set. This approach allows us to treat FSI problems with free bodies and large deformations. This is the main advantage of this method compared to interface tracking methods such as the arbitrary Lagrangian-Eulerian (ALE) method. In the examples the Eulerian approach yields results which are in good agreement with those obtained by the ALE approach. In order to have a 'fair' comparison both methods have been implemented using the same numerical components and software library GASCOIGNE [28].

The full variational formulation of the FSI problem provides the basis for the application of the 'dual weighted residual' (DWR) method for 'goal-oriented' a posteriori error estimation and mesh adaptation. In this method inherent sensitivities of the FSI problem are utilized by solving linear the 'dual' problem.

As a next step, we plan to use the Eulerian approach for FSI problems with large deformations and topology changes. Finally, we intend to extend the variational Eulerian approach and the DWR method to the optimal control of FSI systems.

7 Acknowledgement

This work has been supported by the Deutsche Forschungs Gemeinschaft (DFG, Research Unit 493). This support is gratefully acknowledged.

REFERENCES

[1] W. Bangerth and R. Rannacher, *Adaptive Finite Element Methods for Differential Equations*, Birkhäuser, 2003.

[2] R. Becker and M. Braack, A finite element pressure gradient stabilization for the Stokes equations based on local projections, *Calcolo* 38, 173-199 (2001).

[3] R. Becker and M. Braack, A two-level stabilization scheme for the Navier-Stokes equations, *Proc. ENUMATH-03*, pp. 123-130, Springer, 2003.

[4] R. Becker and R. Rannacher, An optimal control approach to error estimation and mesh adaption in finite element methods, *Acta Numerica 2000* (A. Iserles, ed.), pp. 1-101, Cambridge University Press, 2001.

[5] R. Becker and R. Rannacher, A feed-back approach to error control in finite element methods: basic analysis and examples, *East-West J. Numer. Math.* 4, 237-264 (1996).

[6] M. O. Bristeau, R. Glowinski, and J. Periaux, Numerical methods for the Navier-Stokes equations, *Comput. Phys. Rep.* 6, 73-187 (1987).

[7] G. Carey and J. Oden, *Finite Elements, Computational Aspects*, volume III. Prentice-Hall, 1984.

[8] Y. C. Chang, T. Y. Hou, B. Merriman, and S. Osher, A level set formulation of Eulerian interface capturing methods for incompressible fluid flows, *J. Comp. Phys.* 123, 449-464 (1996).

[9] Th. Dunne. *Adaptive Finite Element Simulation of Fluid Structure Interaction Based on an Eulerian Formulation*, Institute of Applied Mathematics, University of Heidelberg, doctoral dissertation, 2006, in preparation.

[10] Th. Dunne and R. Rannacher, Adaptive Finite Elements Approximation of Fluid-Structure Interaction Based on an Eulerian Variational Formulation In H.-J. Bungartz and M. Schäfer, editors, *Fluid-Structure Interaction: Modelling, Simulation, Optimisation.* to appear in Springer's LNCSE-Series.

[11] R. Glowinski. Finite element methods for incompressible viscous flow, in *In Handbook of Numerical Analysis Volume IX: Numerical Methods for Fluids (Part 3)* (P.G. Ciarlet and J.L. Lions, eds), North-Holland, Amsterdam, 2003.

[12] K. Eriksson, D. Estep, P. Hansbo, and C. Johnson, Introduction to adaptive methods for differential equations. *Acta Numerica 1995* (A. Iserles, ed.), pp. 105–158, Cambridge University Press, 1995.

[13] J. Heywood, R. Rannacher, and S. Turek, *Artificial boundaries and flux and pressure conditions for the incompressible Navier-Stokes equations*, Int. J. Numer. Math. Fluids 22, 325–352 (1992).

[14] C. W. Hirt and B. D. Nichols, Volume of Fluid (VOF) method for the dynamics of free boundaries. *Journal of Computational Physics* 39, 201-225 (1981).

[15] J. Hron and S. Turek, Proposal for numerical benchmarking of fluid-structure interaction between an elastic object and laminar incompressible flow. In H.-J. Bungartz and M. Schäfer, editors, *Fluid-Structure Interaction: Modelling, Simulation, Optimisation.* to appear in Springer's LNCSE-Series.

[16] J. Hron and S. Turek, Fluid-structure interaction with applications in biomechanics. In H.-J. Bungartz and M. Schäfer, editors, *Fluid-Structure Interaction: Modelling, Simulation, Optimisation.* to appear in Springer's LNCSE-Series.

[17] A. Huerta and W. K. Liu, Viscous flow with large free-surface motion, *Computer Methods in Applied Mechanics and Engineering*, 1988.

[18] D. D. Joseph and Y. Y. Renardy, *Fundamentals of two-fluid dynamics. Part I and Part II*, Springer, New York, 1993. Math. Theory and Applications.

[19] A. Legay, J. Chessa, and T. Belytschko, An Eulerian-Lagrangian method for fluid-structure interaction based on level sets, *Comp. Meth. in Applied Mech. and Engrg.*, accepted, 2004.

[20] S. Osher and J. A. Sethian, Propagation of fronts with curvature based speed: algorithms based on Hamilton-Jacobi formulations, *Journal of Computational Physics* 79, 12 (1988).

[21] R. Rannacher, Finite element methods for the incompressible Navier-Stokes equations, in *Fundamental Directions in Mathematical Fluid Mechanics* (G. P. Galdi, J. Heywood, R. Rannacher, eds), pp. 191–293, Birkhäuser, Basel-Boston-Berlin, 2000.

[22] R. Rannacher, Incompressible Viscous Flow, in *Encyclopedia of Computational Mechanics* (E. Stein, et al., eds), John Wiley, Chichester, 2004.

[23] J.A. Sethian, *Level set methods and fast marching methods.* Cambridge University Press, 1999.

[24] T. E. Tezduyar, M. Behr, and J. Liou, A new strategy for finite element flow computations involving moving boundaries and interfaces the deforming spatial-domain/space-time procedures: I. (The concept and preliminary tests) and II. (Computation of free-surface flows, two-liquid flows and flows with drifting cylinders) *Computer Methods in Applied Mechanics and Engineering*, 1992.

[25] S. Turek, *Efficient solvers for incompressible flow problems: an algorithmic and computational approach*, Springer, Heidelberg-Berlin-New York, 1999.

[26] S. Turek and M. Schäfer, Benchmark computations of laminar flow around a cylinder. In E.H. Hirschel, editor, 'Flow Simulation with High-Performance Computers II', volume 52 of *Notes on Numerical Fluid Mechanics.* Vieweg, 1996.

[27] VISUSIMPLE, An open source interactive visualization utility for scientific computing, `http://visusimple.uni-hd.de/` .

[28] GASCOIGNE, A C++ numerics library for scientific computing, `http://gascoigne.uni-hd.de/` .